Development 139, 1213-1224 (2012) doi:10.1242/dev.071456
© 2012. Published by The Company of Biologists Ltd

RIPPLY3 is a retinoic acid-inducible repressor required for setting the borders of the pre-placodal ectoderm

Amanda Janesick[1], Jason Shiotsugu[1,*], Mao Taketani[1,‡] and Bruce Blumberg[1,2,§]

SUMMARY

Retinoic acid signaling is a major component of the neural posteriorizing process in vertebrate development. Here, we identify a new role for the retinoic acid receptor (RAR) in the anterior of the embryo, where RAR regulates *Fgf8* expression and formation of the pre-placodal ectoderm (PPE). RARα2 signaling induces key pre-placodal genes and establishes the posterolateral borders of the PPE. RAR signaling upregulates two important genes, *Tbx1* and *Ripply3*, during early PPE development. In the absence of RIPPLY3, TBX1 is required for the expression of *Fgf8* and hence, PPE formation. In the presence of RIPPLY3, TBX1 acts as a transcriptional repressor, and functions to restrict the positional expression of *Fgf8*, a key regulator of PPE gene expression. These results establish a novel role for RAR as a regulator of spatial patterning of the PPE through *Tbx1* and RIPPLY3. Moreover, we demonstrate that *Ripply3,* acting downstream of RAR signaling, is a key player in establishing boundaries in the PPE.

KEY WORDS: Patterning, Preplacodal Ectoderm, Retinoic Acid, Ripply3, Tbx1, *Xenopus*

INTRODUCTION

Retinoid signaling acting through the nuclear retinoic acid receptors (RARs) is crucial to the establishment of the anteroposterior (AP) axis during embryonic development. RARs function as ligand-modulated transcription factors that activate expression of their target genes (Chambon, 1996; Mangelsdorf et al., 1995; Mark et al., 2009). Studies in a variety of systems have shown that retinoic acid (RA) is an important component of the neural posteriorizing signal (Blumberg et al., 1997; Durston et al., 1989; Lloret-Vilaspasa et al., 2010; Papalopulu and Kintner, 1996; Shiotsugu et al., 2004) as well as of the AP patterning of the neural crest, somites and limbs (Moreno et al., 2008; Moreno and Kintner, 2004; Niederreither et al., 2002; Stratford et al., 1999; Villanueva et al., 2002). Retinoid signaling also establishes AP identity in the endoderm and mesoderm (Bayha et al., 2009; Deimling and Drysdale, 2009; Pan et al., 2007).

RAR signaling has been studied in some detail in the neural crest (Dupe and Pellerin, 2009; Li et al., 2010; Villanueva et al., 2002); RA is required for eye morphogenesis, otocyst development and specification of the olfactory epithelium (Bok et al., 2011; Lupo et al., 2011; Matt et al., 2005; Radosevic et al., 2011; Rawson and LaMantia, 2006; Romand et al., 2006). Relatively little is known about RAR function in the early patterning of sensory organs of the head. The pre-placodal ectoderm (PPE) is an anterior lateral crescent-shaped region that forms at the boundary of the neural plate and neural crest (Brugmann and Moody, 2005; Moody, 2007; Schlosser and Ahrens, 2004). Sensory placodes are epidermal thickenings derived from the PPE that give rise to characteristic sensory organs (e.g. olfactory, lens and otic placodes) and specialized ganglia (e.g. trigeminal, profundal, epibranchial and otic) of the vertebrate head (Ahrens and Schlosser, 2005; David et al., 2001; Schlosser and Ahrens, 2004). Much is known about the molecular pathways that subdivide the PPE into individual sensory placodes and how these give rise to adult structures. Less is known about the mechanisms through which the PPE is established and segregated from the adjacent neural crest. Whether the PPE is derived from a common precursor shared with neural crest (Brugmann and Moody, 2005; Streit, 2007) or is instead a distinct entity with a different origin (Ahrens and Schlosser, 2005; Pieper and Schlosser, 2009; Schlosser, 2008) is currently controversial.

Our previous work suggested that RAR is involved in the AP patterning of the PPE. Knockdown of RARα2 led to posterolateral expansion of *Fgf8* and *Fgfr4* expression in the PPE (Shiotsugu et al., 2004). *Fgf8,* together with BMP inhibitors, induces expression of key factors required for placode development (Ahrens and Schlosser, 2005; Litsiou et al., 2005). Therefore, our result suggested that RARα2 is necessary to restrict the posterolateral boundary of the PPE, probably by inducing repressors of *Fgf8/Fgfr4* expression. Our published microarray analysis (Arima et al., 2005) identified two interesting RA-induced genes expressed in the PPE: *Tbx1*, a T-box transcription factor; and *Dscr6*, a novel member of the Ripply/Bowline family, designated as *Ripply3*. Members of the Ripply/Bowline family are *Groucho*-associated co-repressors that regulate regional boundaries of gene expression, via interaction with T-box proteins (Kawamura et al., 2008; Moreno et al., 2008). We hypothesized that RAR signaling controls the borders of *Fgf8* expression in the PPE by regulating the expression of *Ripply3* and *Tbx1*.

Here, we show that RAR signaling is required for the AP patterning of the PPE. RA upregulates *Ripply3* throughout early development, whereas *Tbx1* is upregulated by RA before (in contrast to published findings), but inhibited after, neurogenesis. TBX1 has a dual function in the PPE downstream of RAR. TBX1 induces PPE gene expression in regions where RIPPLY3 is absent. However, TBX1 restricts the posterolateral boundaries of PPE gene expression in areas where its expression overlaps with *Ripply3* along the lateral edge of the anterior crescent demarcating the PPE. RIPPLY3

[1]Department of Developmental and Cell Biology, 2011 Biological Sciences 3, University of California, Irvine, CA 92697-2300, USA. [2]Department of Pharmaceutical Sciences, University of California, Irvine, CA 92697-2300, USA.

*Present address: Cedars-Sinai Medical Center, Research Development, 8700 Beverly Blvd, Los Angeles, CA 90048, USA
‡Present address: Department of Bioengineering and Therapeutic Sciences, University of California San Francisco, Byers Hall 308C, 1700 4th Street, MC 2530, San Francisco, CA 94158, USA
§Author for correspondence (blumberg@uci.edu)

Accepted 4 January 2012

represses the ability of TBX1 to activate reporter gene constructs in vivo and this inhibition depends on the association of RIPPLY3 with its co-repressor GROUCHO and with TBX1. In agreement with our predictions, RIPPLY3 knockdown perturbs the borders of PPE marker expression. These results demonstrate a novel role for RAR in the precise positioning of the PPE boundaries and establish RIPPLY3 as a key factor that demarcates the boundaries of the PPE.

MATERIALS AND METHODS

Ripply3 alignment and construction of a phylogenetic tree

Ripply sequences were obtained from Genbank and Uniprot databases (Benson et al., 2008; Uniprot Consortium, 2009), aligned with MAFFT (L-INS-i algorithm) (Katoh et al., 2009; Katoh et al., 2005) and a phylogenetic tree constructed with PROml, version 3.69 (Protein Maximum Likelihood) (Felsenstein, 2005). Default settings were used, global rearrangements (–G) were performed, and the outgroup (–O) was set to amphioxus. The resultant tree was drawn with FigTree (Rambaut, 2007). Conserved domains of the Ripply gene family were visualized with WebLogo (Crooks et al., 2004; Schneider and Stephens, 1990).

Embryos

Xenopus eggs were fertilized in vitro as described previously (Blumberg et al., 1997; Koide et al., 2001) and embryos staged according to Nieuwkoop and Faber (Nieuwkoop and Faber, 1967). Embryos were maintained in 0.1× MBS until appropriate stages or treated with 1 μM agonist (TTNPB) and 1 μM antagonist (AGN193109) as described (Arima et al., 2005).

Microinjection

Embryos were injected bilaterally or unilaterally at the two-cell stage with combinations of gene specific morpholinos (MO), mRNAs and 100 pg/embryo β-galactosidase mRNA lineage tracer. MOs used for this study are found in supplementary material Table S1. Control embryos were injected with 20 ng standard control MO: CCT CTT ACC TCA GTT ACA ATT TAT A (GeneTools). The following plasmids were constructed by PCR amplification of the protein-coding regions of the indicated genes and cloning into the expression vector pCDG1: x*RARa2.2* (Sharpe, 1992), x*Tbx1* (Ataliotis et al., 2005) and x*Ripply3* (Hitachi et al., 2009). x*Ripply3*$^{WRPW\rightarrow AAAA}$, x*Ripply3*$^{FPVQ\rightarrow AAAA}$ and *Ripply3*$^{WRPW\rightarrow AAAA,\ FPVQ\rightarrow AAAA}$ were constructed by two-fragment PCR and cloned into pCDG1. pCS2-*mCherry* was provided by Dr Thomas Schilling (University of California, Irvine, CA, USA). All pCDG1 plasmids were linearized with *Not*I and mRNA was transcribed using mMessage mMachine T7 (Ambion). pCS2-*mCherry* was linearized with *Not*I and transcribed using mMessage mMachine SP6 (Ambion).

Whole-mount in situ hybridization

Whole-mount in situ hybridization was performed as described previously (Blumberg et al., 1997; Koide et al., 2001). *Six1* (courtesy of Sally Moody, George Washington University, Washington DC, USA) was cloned into pBluescript II SK and linearized with *Bam*HI. *Fgf8* (courtesy of Nancy Papalopulu, University of Manchester, UK) cloned into pCS2 was linearized with *Bam*HI. *Ripply3* (clone Xl018m04) was linearized with *Not*I and transcribed with T7 RNA polymerase. *Tbx1*, *Eya1* and *Sox3* probes were prepared via PCR amplification of coding regions from cDNA: x*Tbx1* (Ataliotis et al., 2005), x*Eya1* (David et al., 2001) and *xSox3* (Koyano et al., 1997). A T7 promoter was added to the 3′ end and probes were transcribed with MEGAscript T7 (Ambion) in the presence of digoxigenin-11-UTP or dinitrophenol-11-UTP as previously described (Arima et al., 2005). Forward primers and reverse primers containing a T7 promoter are listed in supplementary material Table S2. For double whole-mount in situ hybridization, genes were visualized with BM Purple (Roche) and either Fast Red (Roche) in 0.1 M Tris (pH 8.2) or BCIP (0.1875 mg/ml) and Tetrazolium Blue (0.5 mg/ml) in 100 mM Tris (pH 9.5), 50 mM $MgCl_2$, 100 mM NaCl and 2 mM levamisol. The first alkaline-phosphatase conjugated antibody was deactivated by washing embryos with 0.1 M glycine (pH 2) and 0.1% Tween for 40 minutes. The embryos were washed (four times, 20 minutes each) with MAB before staining for the second gene proceeded.

QPCR

Total embryo RNA was extracted using Trizol reagent (InVitrogen Life Technologies), DNAse treated, LiCl precipitated and then reverse transcribed using Superscript III reverse transcriptase according to the manufacturer-supplied protocol (InVitrogen Life Technologies). The resultant first-strand cDNA was diluted 10-fold, then amplified and quantitated using a DNA Engine Opticon Continuous Fluorescence Detection System (Bio-Rad) with SYBR green detection (Roche Applied Science). Primer sets used are listed in supplementary material Table S3. Each primer set amplified a single band by gel electrophoresis and melting curve analysis. QPCR data was analyzed by employing the ΔΔCt method (Livak and Schmittgen, 2001) normalizing to *Histone H4*, which is insensitive to retinoic acid (Arima et al., 2005). Mann-Whitney statistical analysis was performed using MATLAB.

Embedding and sectioning

Embryos from whole-mount in situ hybridization were cleared with Histoclear and embedded in Paraplast+ using Sakura Finetek disposable base molds (15 mm × 15 mm × 5 mm) and yellow embedding rings. Serial sections were mounted onto Superfrost+ microscope slides, dried overnight, then dewaxed with xylene and photographed.

Luciferase assay

Two copies of the Brachyury T-box sites were cloned into tk-luc (Glass et al., 1989) using primers shown in supplementary material Table S4 via *Exo*III digestion (Li and Evans, 1997) into the *Hin*dIII and *Bam*HI sites of pTK-luc. Embryos derived from the same frog were injected at the two-cell (2/2 blastomeres) or four-cell stage (4/4 blastomeres), with 50 pg TBRE-TK-Luc (WT or MUT) construct and specific amounts and combinations of *Tbx1* mRNA, *Ripply3* mRNA or *Ripply3*$^{WRPW\rightarrow AAAA,\ FPVQ\rightarrow AAAA}$ mRNA (indicated in Fig. 9). *mCherry* mRNA was added to each injection solution to keep the total amount of mRNA constant. Embryos were allowed to develop until stage 11, and then homogenized in 10 μl/embryo lysis buffer [0.1 M phosphate (pH 7.2), 1 mM DTT, 0.4 mM AEBSF], by two cycles of freeze thawing interspersed with vigorous mixing. A Bradford assay (BioRad) determined total protein concentration. Sodium luciferin solution (100 μl; 1× luciferase base buffer, 0.5 mM ATP, 5 mM DTT, 0.15 mg/ml coenzyme A, 0.5 mM sodium luciferin) and 20 μl of cleared lysate were added to a 96-well plate in triplicate. Relative light units were measured using an ML3000 luminometer, then normalized to total protein (Milnes et al., 2008). Error bars represent biological replicates (multiple pools of five embryos derived from the same female frog).

RESULTS

Tbx1 and *Ripply3*/*DSCR6* are expressed in the PPE

Previous results showed that RARα2 knockdown led to a posterolateral expansion of *Fgf8* expression in the *Xenopus* neurula that was rescued by co-injection of *Rarα2* mRNA (Shiotsugu et al., 2004) (supplementary material Fig. S1). Our microarray study identified two RAR target genes, *Tbx1* and *DSCR6*/*Ripply3*, expressed in the PPE that we hypothesized might restrict *Fgf8* expression (Arima et al., 2005). Whole-mount in situ hybridization revealed that *Tbx1* and *Ripply3*/*DSCR6* are expressed in the early PPE (Fig. 1A,B). Expression is ubiquitous until stage 16, when specific staining begins to occur at the horns of the anterior crescent. *Ripply3* separates into a PPE domain circumscribed by intermediate and lateral plate mesoderm (Fig. 1B, stage 20, inset). Both genes are expressed in the epibranchial placodes (Fig. 1A,B; supplementary material Fig. S2) of tailbud embryos. *Tbx1* is also expressed in the otic placode, whereas *Ripply3* is expressed in the pronephros. Similar results were reported for *Tbx1* (Ataliotis et al., 2005; Showell et al., 2006) and for *Ripply3* (Hitachi et al., 2009). Quantitative real-time RT-PCR (QPCR) analysis showed that *Ripply3* is expressed maternally. Zygotic transcription of both *Ripply3* and *Tbx1* first becomes prominent in the early neurula and continues to be expressed until tailbud stages (Fig. 1C,D).

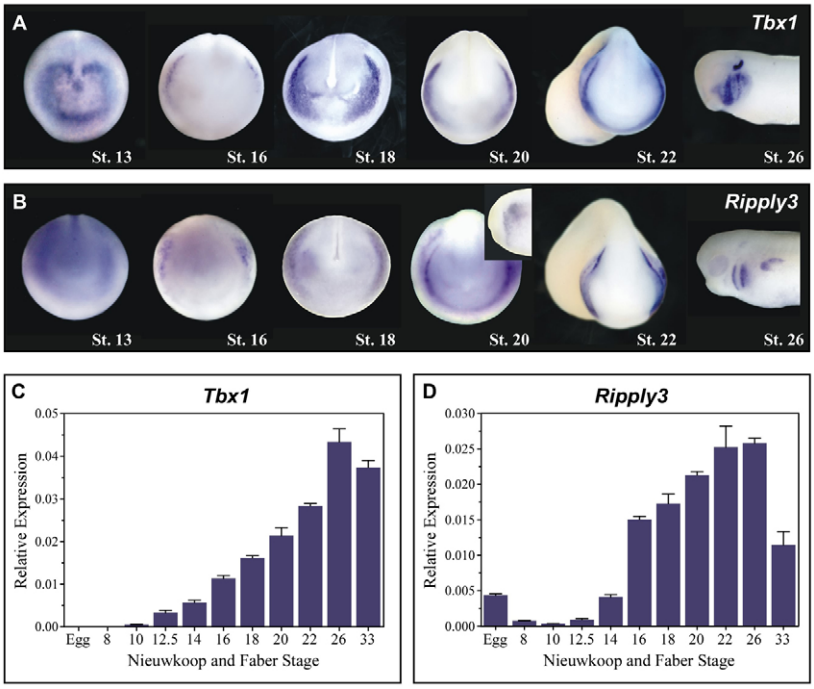

Fig. 1. Expression of *Tbx1* and *Ripply3* across developmental time. (**A**,**B**) Whole-mount in situ hybridization of *Tbx1* (A) and *Ripply3* (B) gene expression at Nieuwkoop and Faber developmental stages 13, 16, 18, 20, 22 and 26 (B). (**C**) QPCR showing *Tbx1* gene expression over developmental time. (**D**) QPCR showing *Ripply3* gene expression over developmental time. In C and D, the *y*-axis represents $2^{-\Delta Ct}$ values normalized to the housekeeping gene *histone H4*.

Ripply3 belongs to the *Ripply*/*Bowline* family

RIPPLY3 has two highly conserved regions found in all Ripply family genes: a WRPW motif and a C-terminal *Ripply* homology domain (also called the bowline-DSCR-Ledgerline conserved 'BDLC' region) (Kondow et al., 2006). The WRPW motif facilitates interaction with GROUCHO (Fisher et al., 1996; Paroush et al., 1994). The 'BDLC' domain (supplementary material Fig. S3A) is predicted to mediate contacts with T-box proteins (Kawamura et al., 2008).

We aligned the available full-length sequences from Ripply genes and then generated a phylogenetic tree using the PROml maximum likelihood-based method (Felsenstein, 2005) (Fig. 2). The resulting tree properly segregates the three Ripply families. *X. laevis Ledgerline* and *Bowline* belong to the *Ripply2* family, and there are two corresponding *X. tropicalis* genes (*Ripply2.1=Ledgerline*; *Ripply2.2=Bowline*), which are adjacent on scaffold 8, suggesting a local duplication event. As *X. tropicalis* is a true diploid organism, the similarities between *Ripply2.1* and *Ledgerline*, and *Ripply2.2* and *Bowline* suggest that these *X. laevis* genes are not pseudo-alleles resulting from pseudo-tetraploidy of *X. laevis*, but rather are distinct genes. In support of this, we identified the tetraploid copies of *Ledgerline* and *Bowline* (supplementary material Fig. S3B) and these are labeled as 2.1A and 2.1B, and 2.2A and 2.2B in Fig. 2. We were unable to identify a *Xenopus Ripply1* ortholog and propose that the duplicated *Ripply2* genes may subsume its function. To date, Ripply sequences are only found in Deuterostomes, with the exception of the sea anemone *Nematostella vectensis* (Nv genome v1.0, scaffold_76:151284-156895).

RAR is required for *Tbx1* and *Ripply3* expression

Research in several laboratories has linked RA with *Tbx1* expression, albeit not in the PPE. Studies using mouse and zebrafish embryos demonstrated that application of high concentrations of RA leads to downregulation of *Tbx1*. Hence, the prevailing view is that endogenous RA inhibits the expression of *Tbx1* in vitro and in vivo (Ataliotis et al., 2005; Guris et al., 2006; Roberts et al., 2005; Zhang et al., 2006). Our microarray results revealed that *Tbx1* was upregulated by RA treatment in stage 15-18 (neurula) *Xenopus laevis* embryos (Arima et al., 2005). Time course experiments resolved this seemingly contradictory effect; the RAR-selective agonist TTNPB induced expression of *Tbx1* prior to the late neurula (stage 18), but *Tbx1* levels were downregulated at subsequent time points (Fig. 3A). Hence, the current view that *Tbx1* is repressed by RA depends on when the expression is analyzed. *Ripply3* showed consistent induction by TTNPB, and repression by the RAR-selective antagonist AGN193109 throughout early development (Fig. 3B).

These results establish that *Ripply3* expression and early *Tbx1* expression are stimulated by RA in the PPE. We tested for the necessity of RA signaling by unilaterally microinjecting embryos with a morpholino oligonucleotide (MO) directed against *Rarα2* (*Rarα2* MO). Whole-mount in situ hybridization at neurula stages revealed that expression of *Tbx1* and *Ripply3* was strongly downregulated in the injected side (Fig. 4B,E). MO specificity was demonstrated by rescuing the phenotype with *Rarα2* mRNA (Fig. 4C,F). Thus, RARα2 is essential for correct expression of *Tbx1* and *Ripply3* in the PPE.

Next, we asked whether RARα2 knockdown would affect *Eya1* and *Six1*, known markers of the PPE (Litsiou et al., 2005; Schlosser and Ahrens, 2004). *Eya1* and *Six1* expression was inhibited by *Rarα2* MO (Fig. 4H,K) and rescued by *Rarα2* mRNA (Fig. 4I,L). In partial knockdown embryos, where *Eya1* and *Six1* were mildly visible on the injected side, there was a posterolateral shift in their expression (not shown). We would expect the boundaries of *Eya1* and *Six1* to be shifted by partial RARα2 loss of function because this leads to a posterolateral shift of the *Fgf8* expression border (supplementary material Fig. S1) (Shiotsugu et al., 2004). More complete RARα2 loss of function should lead to loss of *Eya1* and *Six1* expression as discussed below. These results demonstrate that RARα2 is crucial to restrict the border of *Fgf8* and is a positive regulator of *Eya1* and *Six1* expression.

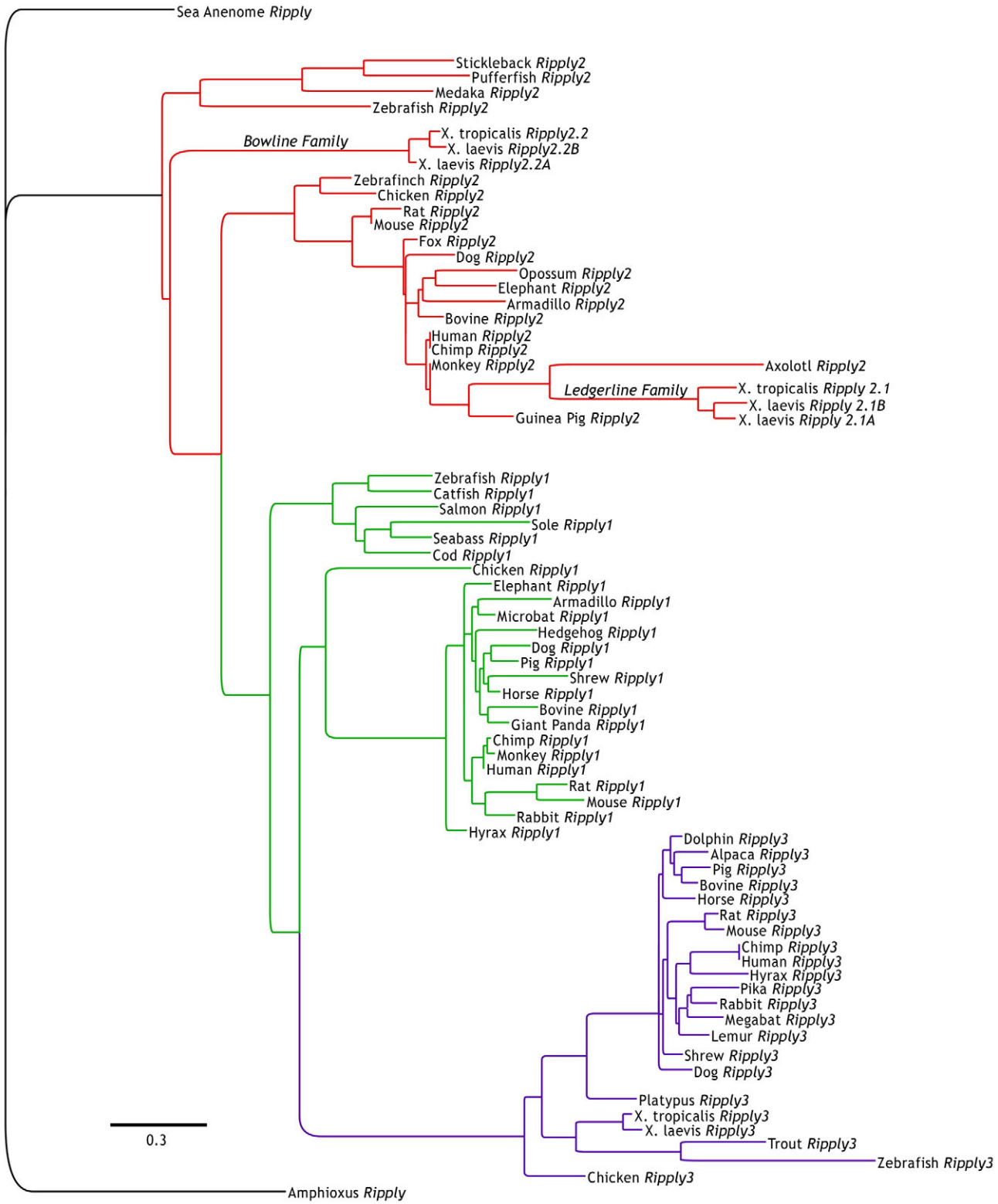

Fig. 2. Ripply phylogenetic tree. Phylogenetic tree of Ripply sequences (aligned with MAFFT) generated using the PROml maximum likelihood-based method with global rearrangements. The scale bar represents the divergence distance of 0.3 amino acid substitutions per site of the *Ripply* sequence.

Double whole-mount in situ hybridization reveals spatial relationship of PPE genes

We performed double whole-mount in situ hybridization to ascertain the spatial relationships between *Ripply3* and other PPE genes. The *Ripply3* expression domain skirts the lateral edge of the anterior crescent occupied by *Tbx1* (Fig. 5A, Fig. 6A) and *Fgf8* (Fig. 5D, Fig. 6D). *Tbx1* significantly overlaps with *Ripply3* (Fig. 5A, Fig. 6A) and *Fgf8* (Fig. 5E, Fig. 6E); however, expression of *Ripply3* and *Fgf8* do not overlap (Fig. 5D, Fig. 6D). *Ripply3* expression is not contiguous with *Six1*, and would probably not directly confine its posterolateral

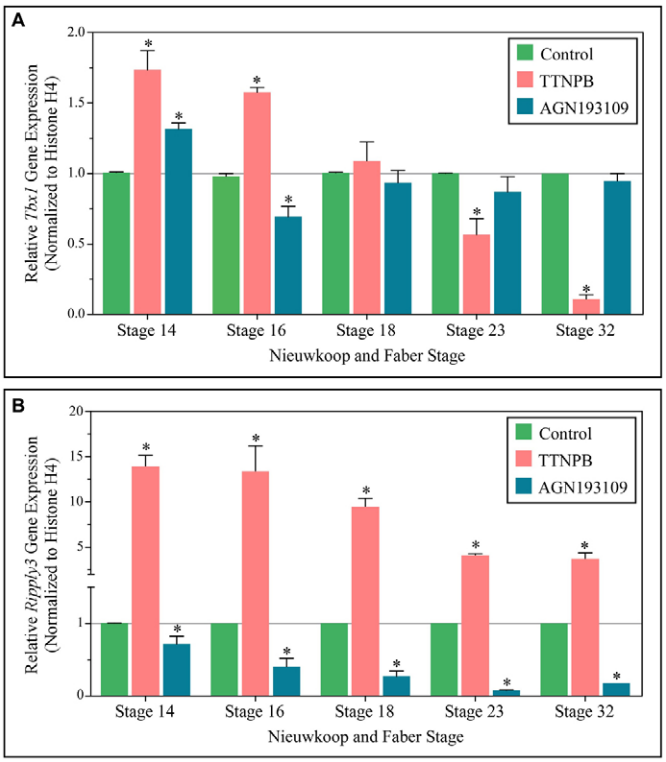

Fig. 3. *Tbx1* and *Ripply3* expression are modulated by TTNPB and AGN193109 treatments. (**A**,**B**) QPCR of *Tbx1* (A) and *Ripply3* (B) expression from whole embryos treated with TTNPB (RAR-specific agonist), AGN193109 (RAR-specific antagonist) or control vehicle (0.1% ethanol). The *y*-axis represents fold induction relative to solvent control value at each stage. $2^{-\Delta\Delta Ct}$ values were normalized to *histone H4*. Asterisks represent differences between control and treated embryos that were statistically significant ($P<0.05$). (A) *Tbx1* is induced by TTNPB early, and repressed by TTNPB in later stages. (B) *Ripply3* is induced by TTNPB and repressed by AGN193109 across all developmental stages.

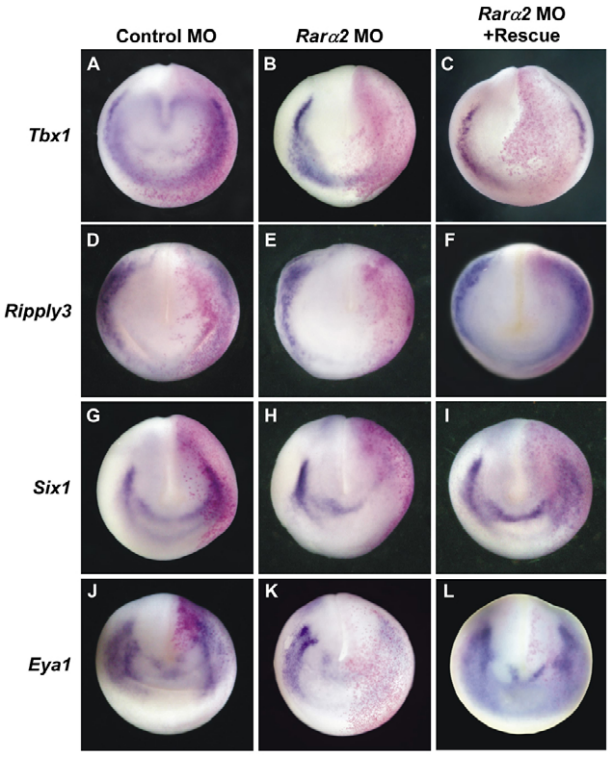

Fig. 4. RARα2 is required for expression of PPE genes. Embryos were injected unilaterally at the two- or four-cell stage. The injected side is on the right, as indicated by the magenta β-galactosidase lineage tracer staining. (**A**,**D**,**G**,**J**) Control expression of *Tbx1*, *Ripply3*, *Six1* and *Eya1*. (**B**,**E**,**H**,**K**) 10 ng *RARα2* MO reduced expression of *Tbx1* (14/15 embryos), *Ripply3* (9/10), *Six1* (6/11) and *Eya1* (8/9). (**C**,**F**,**I**,**L**) 10 ng *RARα2* MO + 0.5 ng *RARα2* mRNA rescued expression of *Tbx1* (5/11 embryos), *Ripply3* (8/11), *Six1* (11/14) and *Eya1* (13/17).

border (Fig. 5B, Fig. 6B). *Tbx1* overlaps *Six1* in the horns of the crescent but not the arc (Fig. 5F, Fig. 6F). *Eya1* has two PPE expression domains: the posterior placodal (pp) area and the profundal placodal (pPrV) area (David et al., 2001). *Ripply3* and *Tbx1* expression overlap with the former, but not with the latter (Fig. 5C,G, Fig. 6C,G). *Fgf8* expression parallels the expression of *Six1*, except in the bottom of the crescent (where *Fgf8* expression is lateral to *Six1*). *Fgf8* expression is largely localized between the pp and pPrV domains of *Eya1*, although there is some overlap of expression (supplementary material Fig. S4). We infer from these expression patterns that RIPPLY3 and TBX1 influence *Six1* and *Eya1* indirectly, probably via *Fgf8*. Fig. 6H summarizes the expression domains of the PPE genes tested in Figs 5 and 6.

Fgf8 establishes the PPE, but TBX1 maintains *Fgf8* expression

Fgf8 is essential for establishing the PPE (reviewed in Moody, 2007) where it also mediates *Eya1* and *Six1* expression (Ahrens and Schlosser, 2005). Hence, it was not surprising that MO-mediated knockdown of FGF8 (leading to 70% reduction in *Fgf8* mRNA levels; supplementary material Fig. S5) decreased *Tbx1* and *Ripply3* expression (Fig. 7B,D). TBX1 knockdown resulted in a reduction of *Fgf8*, *Ripply3*, *Six1* and *Eya1* (Fig. 7E,G,I,K) that was rescued with *Tbx1* mRNA (Fig. 7F,H,J,L). QPCR analysis of embryos uniformly injected with the *Tbx1*-MO also revealed reduced expression of PPE genes (supplementary material Fig. S6). Hence, although *Fgf8* induces *Tbx1* and other PPE genes, TBX1 is required to maintain *Fgf8* expression, thus promoting the continued expression of genes within the PPE.

TBX1 is a transcriptional repressor in the presence of RIPPLY3

The results presented above show that *Tbx1* and *Ripply3* are RAR target genes expressed in overlapping patterns in the PPE, supporting the idea that they function together to restrict PPE boundaries. Recently, it was shown in Cos7 cells that TBX1 could repress reporter gene activity in the presence of RIPPLY3 (and that repression was dependent on the WRPW domain), whereas TBX1 would activate reporter gene activity in the absence of RIPPLY3 (Okubo et al., 2011). We tested the effects of *Ripply3* on the ability of *Tbx1* to activate reporter gene constructs in vivo, and whether the effects required the interaction of RIPPLY3 with GROUCHO and TBX1.

No high-affinity TBX1 consensus target DNA sequence has been identified, but most Tbox proteins bind the same core motif, AGGTGTGA (Wilson and Conlon, 2002), which is derived from the

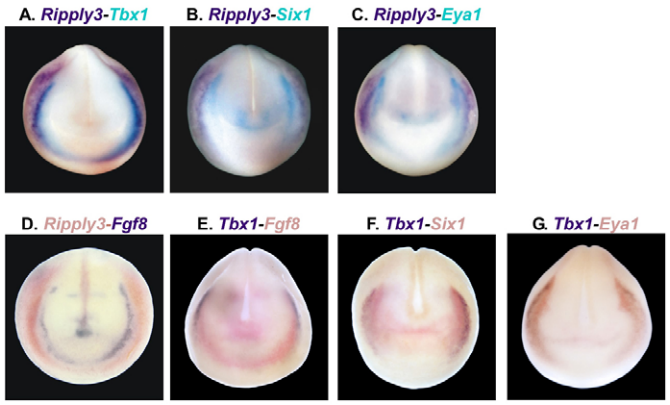

Fig. 5. Double whole-mount in situ hybridization reveals spatial relationship of PPE genes at stage 18. (**A-C**) *Ripply3* (stained with BM Purple) is lateral to *Tbx1*, *Six1* and *Eya1* (stained with BCIP/Tetrazolium Blue), overlapping with *Tbx1* and the posterior placodal (pp) area of *Eya1*. (**D**) *Ripply3* (stained with Fast Red) is lateral to but does not overlap with *Fgf8* (stained with BM-Purple). (**E-G**) *Tbx1* (stained with BM Purple) is lateral to *Fgf8*, *Six1* and *Eya1* (all stained with Fast Red) in stage 18 embryos, overlapping significantly with *Fgf8*, and in the posterior placodal (pp) area of *Eya1*.

consensus Brachyury-binding site (an inverted palindromic repeat of the half-site sequence: AGGT**GTG**AAATT) (Kispert and Herrmann, 1993). The GTG triplet is a key point of protein-DNA contact in the TBX3 crystal structure (Coll et al., 2002). Most T-box proteins bind as monomers, but BRACHYURY and TBX1 dimerize and possess high binding affinity for the palindromic repeat (Muller and Herrmann, 1997; Papapetrou et al., 1997; Sinha et al., 2000).

We created two constructs with *Brachyury* palindromic repeats (one wild type, one mutated) preceding a thymidine kinase minimal promoter, driving firefly luciferase (Fig. 8A). The wild-type construct is expected to bind Tbx1 and associated factors, whereas TBX1 should not bind well to the mutant construct (Fig. 8A). The mutant construct was unresponsive to *Tbx1*, except slightly at the highest dose in injected embryos (supplementary material Fig. S7). The wild-type construct was injected into embryos alone and in combination with *Tbx1*, *Ripply3* or *Ripply3* mutant mRNAs. Microinjected *Tbx1* activated the reporter (Fig. 8B, columns 2 and 6) and co-injection of *Ripply3* repressed luciferase activity (Fig. 8B, columns 3 and 7). This repression was lost when the WRPW and FPVQ domains of RIPPLY3 were mutated (Fig. 8B, columns 4 and 8). Mutation of only the WRPW motif did not consistently relieve repression (data not shown), which suggests that WRPW is not the entire interaction domain. We infer that RIPPLY3 inhibits TBX1-mediated induction of the reporter gene, that RIPPLY3 converts TBX1 from an activator into a repressor and that the ability of RIPPLY3 to inhibit reporter gene activity was dependent upon both its TBX1 and GROUCHO interaction domains.

RIPPLY3 is required to establish the posterolateral boundary of the PPE

Our hypothesis that RIPPLY3 sets the posterolateral border of the PPE predicts that RIPPLY3 knockdown would disrupt this boundary. To test this possibility, we generated two different translation inhibiting MOs (one targeting the 5′ UTR and the other targeting the coding region). These produced similar phenotypes with respect to *Fgf8* expression – a posterolateral shift and a broadening of the expression domain (supplementary material Fig. S8). Owing to the three-dimensional nature of the embryo, a lateral shift in PPE gene expression necessarily also causes a posterior shift. As the phenotypes resulting from combining the *Ripply3* MOs was stronger than individual MOs, all subsequent experiments used the combination.

Ripply3 MO-injected embryos showed a posterolateral shift and expansion in *Fgf8*, *Tbx1*, *Eya1* and *Six1* expression (Fig. 9I-P), compared with the uninjected contralateral side and the control MO-injected embryos (Fig. 9A-H). We quantitated axis length and the extent to which marker gene expression was shifted in *Ripply3* MO-injected embryos (supplementary material Fig. S9). The posterolateral shifts in *Fgf8*, *Tbx1*, *Eya1* and *Six1* expression were significant, whereas the axis length did not differ significantly between the injected and uninjected sides. Therefore, RIPPLY3 is required to establish, or to allow, the formation of a sharp posterolateral boundary of the PPE. We expected to see perceptible changes in the expression of placode markers in *Ripply3* MO-injected tailbud stage embryos. These embryos demonstrated alterations in placode morphology, notably changes in the spacing of the epibranchial placodes, blurring of the lateral line placodes, and altered staining of *Eya1* and *Six1* in and around the otic vesicle (supplementary material Fig. S10). Although the otocyst seems

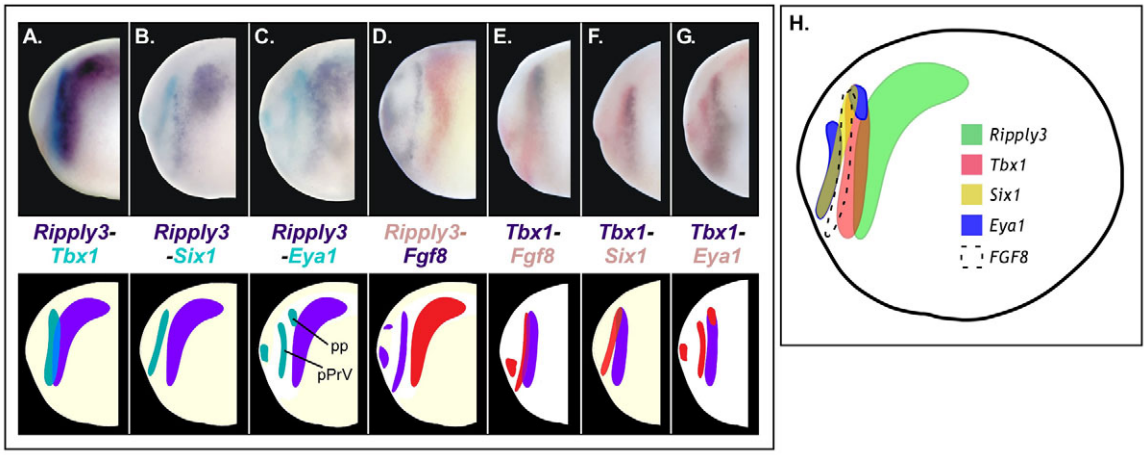

Fig. 6. Lateral view of double wish staining and schematics. (**A-G**) Lateral views of double whole-mount in situ hybridization from Fig. 5, including schematics of the overlapping or non-overlapping PPE genes. pp, the posterior placodal area; pPrV, profundal placodal area. (**H**) Relationship of PPE genes at stage 18.

DEVELOPMENT

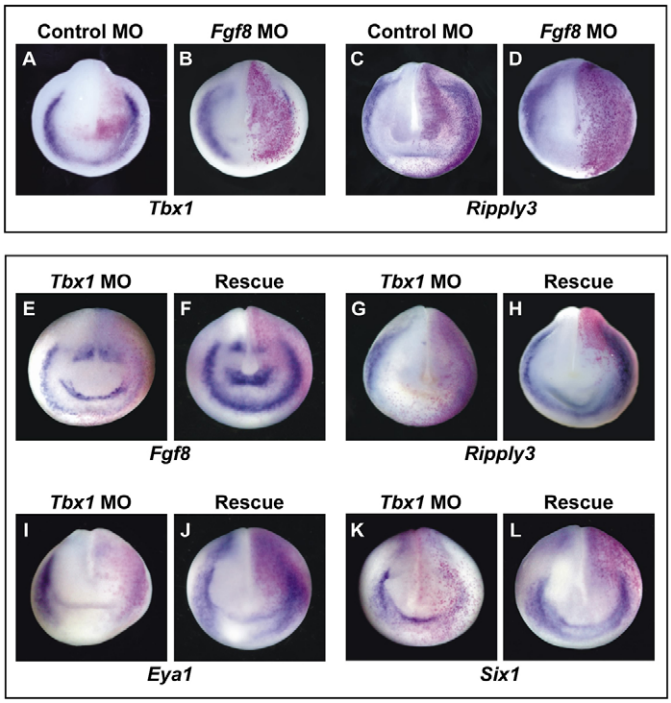

Fig. 7. FGF8 establishes the PPE, but TBX1 maintains *Fgf8* expression. All embryos were injected unilaterally at the two- or four-cell stage. The injected side is on the right. (**A**,**C**) Control expression of *Tbx1* and *Ripply3*. (**B**,**D**) Embryos injected with 30 ng *Fgf8* splice MO; *Tbx1* (8/16 embryos) and *Ripply3* (19/23) expression were knocked down or knocked out. (**E**,**G**,**I**,**K**) Embryos injected with 10 ng *Tbx1* MO showed knockdown of *Fgf8* (12/16 embryos), *Ripply3* (17/21), *Eya1* (21/26) and *Six1* (25/36) expression. (**F**,**H**,**J**,**L**) 10 ng *Tbx1* MO + 0.5 ng *Tbx1* mRNA rescued *Fgf8* (5/8), *Ripply3* (6/8), *Eya1* (6/8) and *Six1* (8/11) expression.

devoid of an otic pit, transverse sections of *Ripply3* MO-injected embryos showed that the otic vesicle is present (supplementary material Fig. S11).

Ripply3 overexpression results in loss of *Tbx1*

Ripply3 is orthologous to the Down Syndrome Critical Region 6 (DSCR6) transcript in humans (Kawamura et al., 2005; Shibuya et al., 2000). Little is known about the function of *DSCR6* in humans or the effects of having three copies of this gene, in the case of Trisomy 21 (Down Syndrome). In human DiGeorge Syndrome, 22q11.2, a region carrying *TBX1*, is deleted. We mimicked the increased dose of DSCR6 in Down Syndrome by microinjecting *Ripply3* mRNA into *Xenopus* embryos. We found that *Tbx1* expression was lost (Fig. 10A,B); however, when the WRPW or FPVQ domain was mutated (*Ripply3*$^{WRPW\rightarrow AAAA}$ or *Ripply3*$^{FPVQ\rightarrow AAAA}$), *Tbx1* expression was essentially normal (Fig. 10C-F). This confirms that the function of RIPPLY3 is dependent on both the WRPW domain (GROUCHO interaction) and the FPVQ domain (TBX1 interaction) (Fig. 8).

DISCUSSION

Tbx1 and *Ripply3*/*DSCR6* are expressed in the PPE and regulated by RA

We identified two genes expressed in the PPE that are induced by RA and require RARα2 in the *Xenopus* neurula: *Tbx1* and *Ripply3*. *Tbx1* is a T-box gene that functions primarily as a transcriptional activator to regulate the expression of target genes such as *Fgf8*, *Fgf10*, *Pitx2*, *Foxa2* and *Gbx2*, which are important in craniofacial patterning, and development of the aortic arches, thymus and parathyroid glands (Ataliotis et al., 2005; Hu et al., 2004; Ivins et al., 2005; Nowotschin et al., 2006; Packham and Brook, 2003). Disruption of *Tbx1* results in placode and pharyngeal defects. For example, the zebrafish mutation, *van gogh* (*Tbx1*) has small otic vesicles owing to an underdeveloped placode (Whitfield et al., 1996). *Xenopus Ripply3* is orthologous to human *DSCR6* and belongs to the Ripply/Bowline gene family. *Ripply3* is primarily associated with the development of the thymus, parathyroid and thyroid gland in mice (Okubo et al., 2011) but it is notable that Down Syndrome is associated with defects in sensory organs. We demonstrate a novel role for RIPPLY3 in regulating the boundaries of the PPE, with TBX1 being an integral player in this process, downstream of RA signaling.

Tbx1 and *Ripply3* are expressed in the anterior lateral crescent that marks the PPE (Fig. 1). *Ripply3* is lateral to *Tbx1*, but they significantly overlap at stage 18 (Figs 5, 6), which led us to investigate interactions between these genes in PPE development. At later stages, *Tbx1* and *Ripply3* are expressed in the epibranchial placodes (supplementary material Fig. S2), which are derived from the PPE, and give rise to cranial sensory neurons. *Tbx1* is also expressed in the otic placode (Ataliotis et al., 2005; Vitelli et al., 2003). *Ripply3* is also expressed in the lateral plate and intermediate mesoderm (Fig. 1), and, subsequently, the pronephros (supplementary material Fig. S2). *DSCR6* is expressed in the human fetal kidney and fetal brain (Shibuya et al., 2000).

We were initially surprised when our microarray results revealed that *Tbx1* was upregulated by RA at neurula stages, contrary to publications showing that *Tbx1* expression is inhibited by RA (Zhang et al., 2006). We found that suppression of *Tbx1* by RA occurs in later stages of embryonic development, whereas early (post-gastrulation) expression of *Tbx1* is upregulated by RA (Fig. 3A). This is supported by evidence demonstrating that early *Tbx1* expression is perturbed in the absence of RA. For example, in vitamin A-deficient quail embryos, *Tbx1* expression was disturbed early and eventually lost (Roberts et al., 2005). RA bead implants led to strong downregulation of *Tbx1*, but only after 8-12 hours, and de novo protein synthesis was required to achieve full suppression of *Tbx1* expression by RA (Roberts et al., 2005). This suggests that an additional, unidentified, factor(s) is induced by RA and acts as a negative regulator of *Tbx1* expression after neurogenesis.

Ripply3 is also upregulated by RA (Fig. 3B); however, unlike *Tbx1*, the increase in expression is greater and is maintained through later stages of development. In the zebrafish presomitic mesoderm, *Ripply1* and *Ripply2* expression sets somite boundaries and was expanded in the presence of RA (Moreno et al., 2008). The RA-inducibility of *Ripply3* provides further evidence that Ripply family genes are sensitive to RA signaling.

Evolutionary origins of *Ripply* genes

Phylogenetic analysis of *Ripply* sequences (Fig. 2) showed that *Xenopus Ripply3* segregated appropriately with the *Ripply3* family. Although it was believed that *Xenopus Bowline* and *Ledgerline* were divergent duplicated genes in the pseudo-tetraploid genome of *X. laevis*, we found that these genes each corresponded to two distinct genes in the diploid *X. tropicalis*. *Bowline/Ripply2.2* and *Ledgerline/Ripply2.1* each have their own pseudo-allele, designated *Ripply2.1A*, *Ripply2.1B* and *Ripply2.2A*, *Ripply2.2B* (supplementary material Fig. S3B). We remain unable to find a *Xenopus Ripply1* ortholog, suggesting that a duplication and loss

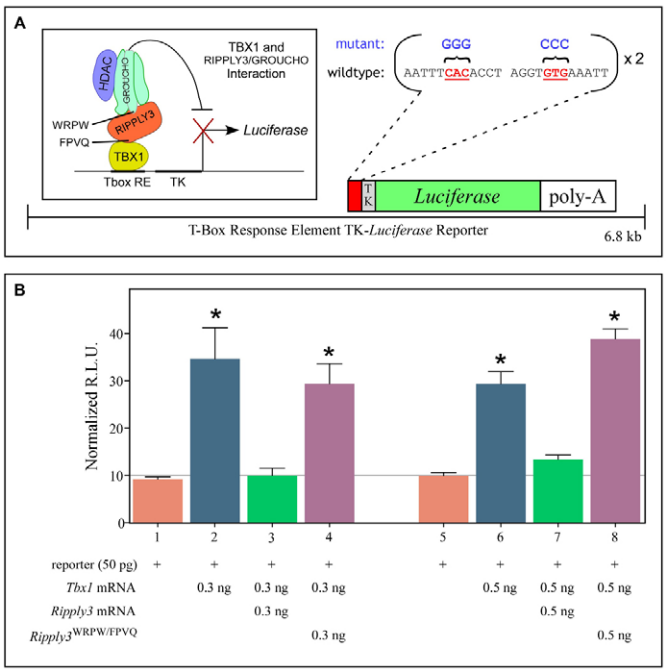

Fig. 8. RIPPLY3 inhibits the ability of TBX1 to activate T-Box response elements. (**A**) Diagram of T-Box response element TK-luciferase reporter (TBRE-TK-Luc). The Brachyury palindromic element is present in two copies, preceding the TK minimal promoter and luciferase. The essential GTG core is indicated in red. Inset: diagram of RIPPLY3, TBX1 and GROUCHO interactions, including the WRPW and FPVQ domains. (**B**) Whole-embryo luciferase assay reflecting *Tbx1* transcriptional activity in the presence or absence of wild-type or mutant *Ripply3*. Relative light units were normalized to total protein (Milnes et al., 2008). Error bars represent biological replicates (multiple pools of five embryos derived from the same female frog). Statistics are relative to reporter alone (*P<0.05). *Tbx1* induces activity about threefold, whereas *Ripply3* represses activity to basal levels when co-injected with *Tbx1*. Microinjection of the mutant *Ripply3*$^{WRPQ→AAAA,\ FPVQ→AAAA}$ mRNA does not repress *Tbx1* induction of reporter activity.

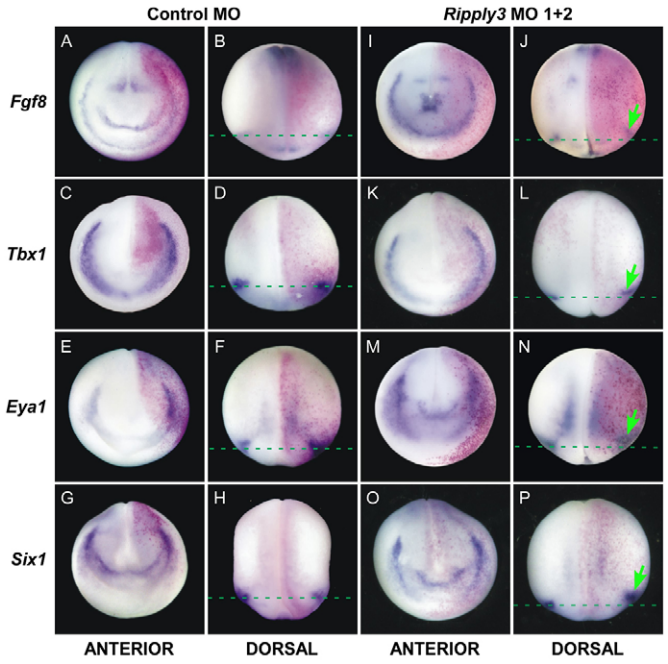

Fig. 9. Knockdown of RIPPLY3 causes posterolateral shift of PPE gene expression. Embryos were injected at the two- or four-cell stage and the injected side is on the right. (**A-H**) Anterior (A,C,E,G) and dorsal (B,D,F,H) views of control expression of *Fgf8*, *Tbx1*, *Eya1* and *Six1*. (**I-P**) Anterior (I,K,M,O) and dorsal (J,L,N,P) views of embryos injected with 50 ng *Ripply3* MO 1+2 showing a posterolateral shift of *Fgf8* (21/29 embryos), *Tbx1* (14/19), *Eya1* (12/18) and *Six1* (12/20).

may have occurred during *Xenopus* evolution. We hypothesize that the *Ripply2.1* and *Ripply2.2* genes have functionally compensated for the lost *Ripply1* gene.

Two intriguing anomalies were noted in the analysis of *Ripply* family genes. First, *Ripply* genes appear only in Deuterostome sequences; however, a likely *Ripply* homolog appears in the genome sequence of the sea anemone *Nematostella vectensis*. No other related sequences appear in any of the other sequenced invertebrate genomes, including *Hydra*, *C. elegans* and *Drosophila*. It is possible that *Ripply* family genes originated before the divergence of Protostomes and Deuterostomes but have subsequently been lost in Protostomes and most Cnidarians. Second, although a *Ripply* gene appears in the Cephalochordate *Branchiostoma floridae*, no *Ripply* genes were identified in the sequenced echinoderm or Urochordate genomes. This would be consistent with an early origin, subsequent loss model.

Expression of *Tbx1* and *Fgf8* is mutually dependent

Several lines of evidence show that FGF signaling acts upstream and downstream of T-box proteins. *Brachyury* was shown to be regulated by FGF signaling, and vice versa, in *Xenopus* mesoderm formation (Casey et al., 1998; Isaacs et al., 1994; Schulte-Merker and Smith, 1995). Zebrafish mutant for the T-box protein *spadetail* showed a reduction in FGF signaling, but inhibition of the FGF receptor exacerbated the *spadetail* phenotype (Griffin and Kimelman, 2003). *Tbx1*-FGF interdependency was also discovered in tooth development (Mitsiadis et al., 2008). Our data support the possibility that *Tbx1* and *Fgf8* are engaged in a regulatory loop in the PPE as *Tbx1* and *Fgf8* expression overlap in the PPE (Figs 5, 6) and knockdown of one gene affects the other (Fig. 7). It is unlikely that *Tbx1* initiates *Fgf8* expression as *Fgf8* expression precedes that of *Tbx1* during development. Therefore, *Tbx1* probably is required for maintenance, rather than induction, of *Fgf8*. As *Fgf8* is required for the expression of *Eya1* and *Six1* (Ahrens and Schlosser, 2005), it follows that *Tbx1* loss of function would indirectly lead to loss of *Eya1* and *Six1*, as we observed (Fig. 7).

RIPPLY3 sets the posterolateral boundary of the PPE

Although much is known about *Tbx1*, *Ripply3* has primarily been studied in the pharyngeal apparatus, and in heart development (Okubo et al., 2011). Zebrafish *Ripply1* (Kawamura et al., 2005), mouse *Ripply2* (Biris et al., 2007; Chan et al., 2007) and *Xenopus Bowline/Ledgerline* (*Ripply2*) (Chan et al., 2006; Kondow et al., 2006) participate in setting somite boundaries during somitogenesis. In *Ripply1* MO-injected zebrafish embryos, somites were not partitioned into distinct divisions (Kawamura et al., 2005; Kawamura et al., 2008). In *Ripply2*$^{-/-}$ mice, the spinal column and ribs were fused, and the caudal myotome had indefinite segmental borders, indicative of defects in early somite segmentation (Chan

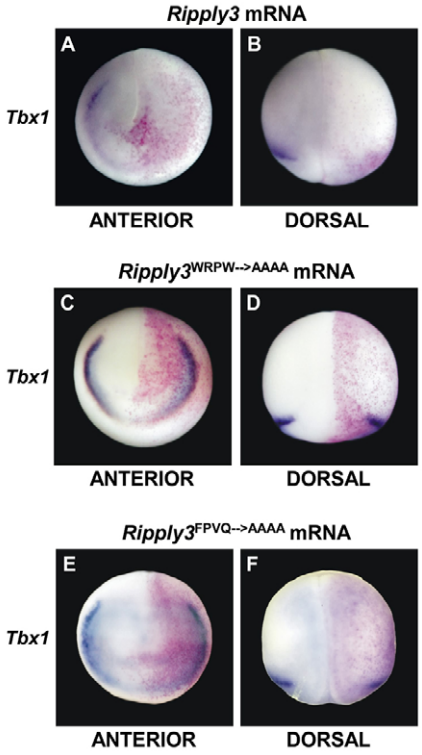

Fig. 10. *Ripply3* gain of function causes loss of *Tbx1* expression. Embryos were injected at the two- or four-cell stage and the injected side is on the right. (**A**,**B**) Anterior (A) and dorsal (B) views of embryos injected with 0.25 ng *Ripply3* mRNA showing a knockdown of *Tbx1* (11/11). (**C**,**D**) Anterior (C) and dorsal (D) views of embryos injected with 0.25 ng *Ripply3*$^{WRPW\rightarrow AAAA}$ mRNA showing no change in *Tbx1* (15/16) expression. (**E**,**F**) Anterior (E) and dorsal (F) views of embryos injected with 0.25 ng *Ripply3*$^{FPVQ\rightarrow AAAA}$ mRNA showing no change in *Tbx1* expression (10/11).

et al., 2007; Morimoto et al., 2007). As other *Ripply* genes appear to function in boundary formation, we hypothesized that *Ripply3* might set or refine the posterolateral border of the PPE.

Ripply3 is spatially positioned to regulate the posterolateral boundary of the PPE because it is expressed lateral to known PPE markers, *Fgf8*, *Eya1* and *Six1*, as well as *Tbx1* (Figs 5, 6). *Ripply3* knockdown led to a posterolateral expansion of *Tbx1*, *Fgf8*, *Eya1* and *Six1* expression boundaries at stage 18 (Fig. 9). RIPPLY2 knockdown caused a similar effect in the presomitic mesoderm, where it caused a shift in *Delta2* and *Thylacine1* expression (Chan et al., 2006). The blurring of somite boundaries led to the fusion of ribs and vertebral components (Chan et al., 2007; Morimoto et al., 2007). RIPPLY3 knockdown led to noticeable changes in placode marker expression in tailbud stage *Xenopus* embryos (supplementary material Fig. S10). The intricate expression patterns of the lateral line, epibranchial and trigeminal placodes became distorted, and the otocyst seemed devoid of an otic pit. However, transverse sections of these embryos showed that the otic vesicle is present in *Ripply3* MO-injected embryos (supplementary material Fig. S11).

Ripply3 does not overlap with *Six1* and *Eya1*; however, *Fgf8* does (Figs 5, 6) and is known to regulate their expression in the PPE (Ahrens and Schlosser, 2005). Thus, the shifts observed in *Six1* and *Eya1* expression in *Ripply3* MO embryos (Fig. 9) probably result from perturbation of the *Fgf8* expression boundary.

RAR regulates *Fgf8* in the PPE through *Ripply3* and *Tbx1*

Mutually inhibitory interactions between RAR and FGF signaling are a common theme in developmental biology (Diez del Corral et al., 2003; Maden, 2006; Niederreither and Dolle, 2008). RA signaling plays crucial roles in the developing lens and otic placodes, in part by regulating *Fgf8* (Bhasin et al., 2003; Mic et al., 2004; Romand et al., 2006; Song et al., 2004) and *Fgf8* regulates components of RA biosynthesis (Mercader et al., 2000; Schneider et al., 2001; Shiotsugu et al., 2004). We have previously explored the relationship of FGF and RARα in the central nervous system in the *Xenopus laevis* embryo (Shiotsugu et al., 2004) and showed that loss of RARα shifted the border of *Fgf8* expression. Knocking down *Ripply3* phenocopied this effect (Fig. 9I,J), suggesting that RIPPLY3 normally restricts the borders of *Fgf8* expression. Because RARα2 is required for *Ripply3* expression (Fig. 4), we hypothesized that *Ripply3* expression is lost in the absence of RAR, and is unable to restrict *Fgf8* expression.

Double whole-mount in situ hybridization revealed that *Ripply3* does not directly overlap with *Fgf8*. As *Tbx1* regulates *Fgf8* (discussed above), we believe that RIPPLY3 regulates *Fgf8* expression via TBX1. Previous studies showed that Ripply proteins convert T-box proteins from transcriptional activators into repressors. *Tbx6* activated the *Thylacine1* promoter and this activation was blunted by co-transfection with *Bowline/Ripply2* and *Groucho* (Kondow et al., 2007). Similarly, *Tbx24*-mediated repression of the *Mesp-b* promoter was conferred by co-expression of *Ripply1/2/3* in luciferase assays (Kawamura et al., 2008). This effect was dependent on the WRPW (required for the Groucho interaction) and FPVQ (required for the T-Box interaction) motifs in RIPPLY, as well as HDAC activity (Kawamura et al., 2008).

We asked whether *Tbx1* transcriptional activity could be reduced by RIPPLY3, and which domains of RIPPLY3 mediated this process. Whole-embryo luciferase assays showed that RIPPLY3 converted *Tbx1* to a transcriptional repressor, and that this was dependent on the WRPW and FPVQ motifs of RIPPLY3 (Fig. 8). Interestingly, *Tbx1* also promoted *Ripply3* expression (Fig. 7). TBX1 knockdown reduced *Ripply3* expression, which is consistent with the observation that *Tbx6* is required for *Bowline/Ledgerline/Ripply2* expression (Hitachi et al., 2008b). TBX6 binds the *Bowline* promoter at a T-Box Response Element (TBRE), in conjunction with THYLACINE1 and E47 to induce expression of *Bowline* (Hitachi et al., 2008b). Thus, in areas where TBX1 is co-expressed with *Ripply3*, their interaction converts TBX1 into a transcriptional repressor that restricts *Fgf8* expression and defines the posterolateral boundary of the PPE. TBX1 further enhances this process by positively regulating *Ripply3*.

Conclusion

Although much is known about the transcriptional cascades that regulate placode identity and the subsequent development of the sensory organs, less is known about the molecular details underlying the initial establishment and patterning of the PPE. The PPE domain is defined specifically in time and space by a combinatorial pattern of signals (BMP, WNT, FGF) (Moody, 2007; Schlosser, 2006; Schlosser, 2008), and we propose that RA signaling through RARα is another important signal in PPE patterning. Accordingly, we further explored the transcriptional mechanisms downstream of RARα in the PPE by asking how RARα regulated expression of two PPE genes: *Tbx1* and *Ripply3*. Fig. 11 summarizes the molecular interactions in PPE formation identified in this paper, together with those previously published by other laboratories.

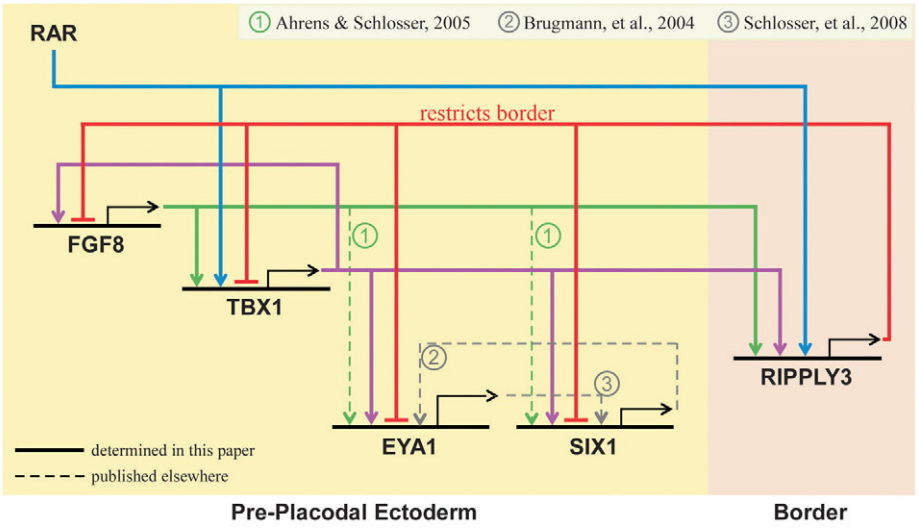

Fig. 11. Wiring diagram of RAR signaling and PPE genes. All interactions found in this paper, and specific to the PPE region, are diagrammed. RAR signaling induces *Tbx1* and *Ripply3* (blue lines). *Ripply3* (red lines) regulates the PPE boundary of *Tbx1*, *Fgf8*, *Six1* and *Eya1* expression. *Tbx1* (purple lines) and *Fgf8* (green lines) engage in a positive-feedback loop, and both are required for *Ripply3*, *Six1* and *Eya1* expression. Previously published PPE interactions are also noted with circled numbers and the pathways indicated by broken lines (Ahrens and Schlosser, 2005; Brugmann et al., 2004; Schlosser et al., 2008).

Precise positioning of the PPE later translates to proper morphological identity of the placodes, thus early border formation is vital. RAR signaling was linked with the regulation of borders, such as in the delineation of somite and rhombomere boundaries, and *Ripply/Bowline* family members set borders in somitogenesis (Biris et al., 2007; Chan et al., 2007; Hitachi et al., 2008a; Kawamura et al., 2005; Kawamura et al., 2008; Moreno et al., 2008; Morimoto et al., 2007). A border-setting gene within the PPE was proposed to exist (Moody, 2007) and we provide in vivo evidence that this is likely to be *Ripply3*. *Ripply3*, which is regulated by RAR, sets the posterolateral border of the PPE, much as other *Ripply* genes do in somite development. It is likely that RAR induces both *Ripply3* and *Tbx1*, which function together to regulate the spatial expression of genes, such as *Fgf8*, along the border of the PPE.

Ripply3 and *Tbx1* are associated with Down Syndrome (DS) and DiGeorge Syndrome, respectively. Intriguingly, DiGeorge Syndrome (caused by a deletion in 22q11.2 containing *Tbx1*) and DS (caused by a trisomy in a large region of chromosome 21 that includes *Ripply3*) share common craniofacial and cardiovascular abnormalities (e.g. small malpositioned ears, flat facial profile, and atrial and septal defects), growth delays (owing to pituitary dysfunction), hearing loss, ocular abnormalities, immunodeficiency (owing to thymic aplasia), and learning disabilities (Korenberg et al., 1994; Ryan et al., 1997). Inner ear defects are common in DS, and most children with DS develop hearing loss (Balkany et al., 1979; Sacks and Wood, 2003; Shott et al., 2001). DS children also have a reduced ability to react to environmental cues and sensory stimuli. Although this is often attributed to cognitive problems related to sensory processing (Bruni et al., 2010; Wuang and Su, 2011), some evidence points to the fact that DS children have impaired tactile, vestibular, nociception and proprioceptive senses (Brandt, 1996; Brandt and Rosen, 1995; Chen and Fang, 2005; Shumway-Cook and Woollacott, 1985). This suggests that early placode defects occur in DS children. Considering the interactions, other researchers and we have demonstrated between RIPPLY3 and TBX1 and the similar phenotypes elicited by *Tbx1* loss of function and *Ripply3* gain of function (Fig. 10), a plausible hypothesis is that the signaling pathways underlying these two diseases converge at the level of TBX1 and RIPPLY3 interaction. Future work will explore the molecular basis of this interaction in vivo and place RIPPLY3, TBX1 and RA signaling in the context of human placode development.

Acknowledgements
We thank Dr Ira Blitz for critical comments on the manuscript. We also thank UCI undergraduate students Sophia Liu and Rachelle Abbey for outstanding technical help in the execution of some experiments.

Funding
Supported by a grant from the National Science Foundation (NSF) [IOS0719576 to B.B.]. A.J. is a pre-doctoral trainee of NSF IGERT DGE 0549479. J.S. was the recipient of a National Institutes of Health National Research Service Award (NRSA) [F32GM073473]. Deposited in PMC for release after 12 months.

Competing interests statement
The authors declare no competing financial interests.

Supplementary material
Supplementary material available online at
http://dev.biologists.org/lookup/suppl/doi:10.1242/dev.071456/-/DC1

References
Ahrens, K. and Schlosser, G. (2005). Tissues and signals involved in the induction of placodal Six1 expression in Xenopus laevis. *Dev. Biol.* **288**, 40-59.
Arima, K., Shiotsugu, J., Niu, R., Khandpur, R., Martinez, M., Shin, Y., Koide, T., Cho, K. W., Kitayama, A., Ueno, N. et al. (2005). Global analysis of RAR-responsive genes in the Xenopus neurula using cDNA microarrays. *Dev. Dyn.* **232**, 414-431.
Ataliotis, P., Ivins, S., Mohun, T. J. and Scambler, P. J. (2005). XTbx1 is a transcriptional activator involved in head and pharyngeal arch development in Xenopus laevis. *Dev. Dyn.* **232**, 979-991.
Balkany, T. J., Downs, M. P., Jafek, B. W. and Krajicek, M. J. (1979). Hearing loss in Down's syndrome. A treatable handicap more common than generally recognized. *Clin. Pediatr.* **18**, 116-118.
Bayha, E., Jorgensen, M. C., Serup, P. and Grapin-Botton, A. (2009). Retinoic acid signaling organizes endodermal organ specification along the entire antero-posterior axis. *PLoS ONE* **4**, e5845.
Benson, D. A., Karsch-Mizrachi, I., Lipman, D. J., Ostell, J. and Wheeler, D. L. (2008). GenBank. *Nucleic Acids Res.* **36**, D25-D30.
Bhasin, N., Maynard, T. M., Gallagher, P. A. and LaMantia, A. S. (2003). Mesenchymal/epithelial regulation of retinoic acid signaling in the olfactory placode. *Dev. Biol.* **261**, 82-98.
Biris, K. K., Dunty, W. C., Jr and Yamaguchi, T. P. (2007). Mouse Ripply2 is downstream of Wnt3a and is dynamically expressed during somitogenesis. *Dev. Dyn.* **236**, 3167-3172.
Blumberg, B., Bolado, J., Jr, Moreno, T. A., Kintner, C., Evans, R. M. and Papalopulu, N. (1997). An essential role for retinoid signaling in anteroposterior neural patterning. *Development* **124**, 373-379.
Bok, J., Raft, S., Kong, K. A., Koo, S. K., Drager, U. C. and Wu, D. K. (2011). Transient retinoic acid signaling confers anterior-posterior polarity to the inner ear. *Proc. Natl. Acad. Sci. USA* **108**, 161-166.
Brandt, B. R. (1996). Impaired tactual perception in children with Down's syndrome. *Scand. J. Psychol.* **37**, 312-316.
Brandt, B. R. and Rosen, I. (1995). Impaired peripheral somatosensory function in children with Down syndrome. *Neuropediatrics* **26**, 310-312.

Brugmann, S. A. and Moody, S. A. (2005). Induction and specification of the vertebrate ectodermal placodes: precursors of the cranial sensory organs. *Biol. Cell* **97**, 303-319.
Brugmann, S. A., Pandur, P. D., Kenyon, K. L., Pignoni, F. and Moody, S. A. (2004). Six1 promotes a placodal fate within the lateral neurogenic ectoderm by functioning as both a transcriptional activator and repressor. *Development* **131**, 5871-5881.
Bruni, M., Cameron, D., Dua, S. and Noy, S. (2010). Reported sensory processing of children with Down syndrome. *Phys. Occup. Ther. Pediatr.* **30**, 280-293.
Casey, E. S., O'Reilly, M. A., Conlon, F. L. and Smith, J. C. (1998). The T-box transcription factor Brachyury regulates expression of eFGF through binding to a non-palindromic response element. *Development* **125**, 3887-3894.
Chambon, P. (1996). A decade of molecular biology of retinoic acid receptors. *FASEB J.* **10**, 940-954.
Chan, T., Satow, R., Kitagawa, H., Kato, S. and Asashima, M. (2006). Ledgerline, a novel Xenopus laevis gene, regulates differentiation of presomitic mesoderm during somitogenesis. *Zoolog. Sci.* **23**, 689-697.
Chan, T., Kondow, A., Hosoya, A., Hitachi, K., Yukita, A., Okabayashi, K., Nakamura, H., Ozawa, H., Kiyonari, H., Michiue, T. et al. (2007). Ripply2 is essential for precise somite formation during mouse early development. *FEBS Lett.* **581**, 2691-2696.
Chen, Y. J. and Fang, P. C. (2005). Sensory evoked potentials in infants with Down syndrome. *Acta Paediatr.* **94**, 1615-1618.
Coll, M., Seidman, J. G. and Muller, C. W. (2002). Structure of the DNA-bound T-box domain of human TBX3, a transcription factor responsible for ulnar-mammary syndrome. *Structure* **10**, 343-356.
Crooks, G. E., Hon, G., Chandonia, J. M. and Brenner, S. E. (2004). WebLogo: a sequence logo generator. *Genome Res.* **14**, 1188-1190.
David, R., Ahrens, K., Wedlich, D. and Schlosser, G. (2001). Xenopus Eya1 demarcates all neurogenic placodes as well as migrating hypaxial muscle precursors. *Mech. Dev.* **103**, 189-192.
Deimling, S. J. and Drysdale, T. A. (2009). Retinoic acid regulates anterior-posterior patterning within the lateral plate mesoderm of Xenopus. *Mech. Dev.* **126**, 913-923.
Diez del Corral, R., Olivera-Martinez, I., Goriely, A., Gale, E., Maden, M. and Storey, K. (2003). Opposing FGF and retinoid pathways control ventral neural pattern, neuronal differentiation, and segmentation during body axis extension. *Neuron* **40**, 65-79.
Dupe, V. and Pellerin, I. (2009). Retinoic acid receptors exhibit cell-autonomous functions in cranial neural crest cells. *Dev. Dyn.* **238**, 2701-2711.
Durston, A. J., Timmermans, J. P., Hage, W. J., Hendriks, H. F., de Vries, N. J., Heideveld, M. and Nieuwkoop, P. D. (1989). Retinoic acid causes an anteroposterior transformation in the developing central nervous system. *Nature* **340**, 140-144.
Felsenstein, J. (2005). PHYLIP (Phylogeny Inference Package) version 3.69 (ed. University of Washington. Distributed by the author. Department of Genome Sciences, Seattle).
Fisher, A. L., Ohsako, S. and Caudy, M. (1996). The WRPW motif of the hairy-related basic helix-loop-helix repressor proteins acts as a 4-amino-acid transcription repression and protein-protein interaction domain. *Mol. Cell. Biol.* **16**, 2670-2677.
Glass, C. K., Lipkin, S. M., Devary, O. V. and Rosenfeld, M. G. (1989). Positive and negative regulation of gene transcription by a retinoic acid-thyroid hormone receptor heterodimer. *Cell* **59**, 697-708.
Griffin, K. J. and Kimelman, D. (2003). Interplay between FGF, one-eyed pinhead, and T-box transcription factors during zebrafish posterior development. *Dev Biol.* **264**, 456-466.
Guris, D. L., Duester, G., Papaioannou, V. E. and Imamoto, A. (2006). Dose-dependent interaction of Tbx1 and Crkl and locally aberrant RA signaling in a model of del22q11 syndrome. *Dev. Cell* **10**, 81-92.
Hitachi, K., Danno, H., Kondow, A., Ohnuma, K., Uchiyama, H., Ishiura, S., Kurisaki, A. and Asashima, M. (2008a). Physical interaction between Tbx6 and mespb is indispensable for the activation of bowline expression during Xenopus somitogenesis. *Biochem. Biophys. Res. Commun.* **372**, 607-612.
Hitachi, K., Kondow, A., Danno, H., Inui, M., Uchiyama, H. and Asashima, M. (2008b). Tbx6, Thylacine1, and E47 synergistically activate bowline expression in Xenopus somitogenesis. *Dev. Biol.* **313**, 816-828.
Hitachi, K., Danno, H., Tazumi, S., Aihara, Y., Uchiyama, H., Okabayashi, K., Kondow, A. and Asashima, M. (2009). The Xenopus Bowline/Ripply family proteins negatively regulate the transcriptional activity of T-box transcription factors. *Int. J. Dev. Biol.* **53**, 631-639.
Hu, T., Yamagishi, H., Maeda, J., McAnally, J., Yamagishi, C. and Srivastava, D. (2004). Tbx1 regulates fibroblast growth factors in the anterior heart field through a reinforcing autoregulatory loop involving forkhead transcription factors. *Development* **131**, 5491-5502.
Isaacs, H. V., Pownall, M. E. and Slack, J. M. (1994). eFGF regulates Xbra expression during Xenopus gastrulation. *EMBO J.* **13**, 4469-4481.
Ivins, S., Lammerts van Beuren, K., Roberts, C., James, C., Lindsay, E., Baldini, A., Ataliotis, P. and Scambler, P. J. (2005). Microarray analysis detects differentially expressed genes in the pharyngeal region of mice lacking Tbx1. *Dev. Biol.* **285**, 554-569.
Katoh, K., Kuma, K., Toh, H. and Miyata, T. (2005). MAFFT version 5, improvement in accuracy of multiple sequence alignment. *Nucleic Acids Res.* **33**, 511-518.
Katoh, K., Asimenos, G. and Toh, H. (2009). Multiple alignment of DNA sequences with MAFFT. *Methods Mol. Biol.* **537**, 39-64.
Kawamura, A., Koshida, S., Hijikata, H., Ohbayashi, A., Kondoh, H. and Takada, S. (2005). Groucho-associated transcriptional repressor ripply1 is required for proper transition from the presomitic mesoderm to somites. *Dev. Cell* **9**, 735-744.
Kawamura, A., Koshida, S. and Takada, S. (2008). Activator-to-repressor conversion of T-box transcription factors by the Ripply family of Groucho/TLE-associated mediators. *Mol. Cell. Biol.* **28**, 3236-3244.
Kispert, A. and Herrmann, B. G. (1993). The Brachyury gene encodes a novel DNA binding protein. *EMBO J.* **12**, 3211-3220.
Koide, T., Downes, M., Chandraratna, R. A., Blumberg, B. and Umesono, K. (2001). Active repression of RAR signaling is required for head formation. *Genes Dev.* **15**, 2111-2121.
Kondow, A., Hitachi, K., Ikegame, T. and Asashima, M. (2006). Bowline, a novel protein localized to the presomitic mesoderm, interacts with Groucho/TLE in Xenopus. *Int. J. Dev. Biol.* **50**, 473-479.
Kondow, A., Hitachi, K., Okabayashi, K., Hayashi, N. and Asashima, M. (2007). Bowline mediates association of the transcriptional corepressor XGrg-4 with Tbx6 during somitogenesis in Xenopus. *Biochem. Biophys. Res. Commun.* **359**, 959-964.
Korenberg, J. R., Chen, X. N., Schipper, R., Sun, Z., Gonsky, R., Gerwehr, S., Carpenter, N., Daumer, C., Dignan, P., Disteche, C. et al. (1994). Down syndrome phenotypes: the consequences of chromosomal imbalance. *Proc. Natl. Acad. Sci. USA* **91**, 4997-5001.
Koyano, S., Ito, M., Takamatsu, N., Takiguchi, S. and Shiba, T. (1997). The Xenopus Sox3 gene expressed in oocytes of early stages. *Gene* **188**, 101-107.
Li, C. and Evans, R. M. (1997). Ligation independent cloning irrespective of restriction site compatibility. *Nucleic Acids Res.* **25**, 4165-4166.
Li, N., Kelsh, R. N., Croucher, P. and Roehl, H. H. (2010). Regulation of neural crest cell fate by the retinoic acid and Pparg signalling pathways. *Development* **137**, 389-394.
Litsiou, A., Hanson, S. and Streit, A. (2005). A balance of FGF, BMP and WNT signalling positions the future placode territory in the head. *Development* **132**, 4051-4062.
Livak, K. J. and Schmittgen, T. D. (2001). Analysis of relative gene expression data using real-time quantitative PCR and the 2(-Delta Delta C(T)) method. *Methods* **25**, 402-408.
Lloret-Vilaspasa, F., Jansen, H. J., de Roos, K., Chandraratna, R. A., Zile, M. H., Stern, C. D. and Durston, A. J. (2010). Retinoid signalling is required for information transfer from mesoderm to neuroectoderm during gastrulation. *Int. J. Dev. Biol.* **54**, 599-608.
Lupo, G., Gestri, G., O'Brien, M., Denton, R. M., Chandraratna, R. A., Ley, S. V., Harris, W. A. and Wilson, S. W. (2011). Retinoic acid receptor signaling regulates choroid fissure closure through independent mechanisms in the ventral optic cup and periocular mesenchyme. *Proc. Natl. Acad. Sci. USA* **108**, 8698-8703.
Maden, M. (2006). Retinoids and spinal cord development. *J. Neurobiol.* **66**, 726-738.
Mangelsdorf, D. J., Thummel, C., Beato, M., Herrlich, P., Schutz, G., Umesono, K., Blumberg, B., Kastner, P., Mark, M., Chambon, P. et al. (1995). The nuclear receptor superfamily: the second decade. *Cell* **83**, 835-839.
Mark, M., Ghyselinck, N. B. and Chambon, P. (2009). Function of retinoic acid receptors during embryonic development. *Nucl. Recept. Signal.* **7**, e002.
Matt, N., Dupe, V., Garnier, J. M., Dennefeld, C., Chambon, P., Mark, M. and Ghyselinck, N. B. (2005). Retinoic acid-dependent eye morphogenesis is orchestrated by neural crest cells. *Development* **132**, 4789-4800.
Mercader, N., Leonardo, E., Piedra, M. E., Martinez, A. C., Ros, M. A. and Torres, M. (2000). Opposing RA and FGF signals control proximodistal vertebrate limb development through regulation of Meis genes. *Development* **127**, 3961-3970.
Mic, F. A., Molotkov, A., Molotkova, N. and Duester, G. (2004). Raldh2 expression in optic vesicle generates a retinoic acid signal needed for invagination of retina during optic cup formation. *Dev. Dyn.* **231**, 270-277.
Milnes, M. R., Garcia, A., Grossman, E., Grun, F., Shiotsugu, J., Tabb, M. M., Kawashima, Y., Katsu, Y., Watanabe, H., Iguchi, T. et al. (2008). Activation of steroid and xenobiotic receptor (SXR, NR1I2) and its orthologs in laboratory, toxicologic, and genome model species. *Environ. Health Perspect.* **116**, 880-885.
Mitsiadis, T. A., Tucker, A. S., De Bari, C., Cobourne, M. T. and Rice, D. P. (2008). A regulatory relationship between Tbx1 and FGF signaling during tooth morphogenesis and ameloblast lineage determination. *Dev. Biol.* **320**, 39-48.
Moody, S. A. (2007). Determination of preplacodal ectoderm and sensory placodes. In *Principles of Developmental Genetics* (ed. S. A. Moody), pp. 1-25. Washington, D.C., USA: Elsevier, Inc.

Moreno, T. A. and Kintner, C. (2004). Regulation of segmental patterning by retinoic acid signaling during Xenopus somitogenesis. *Dev. Cell* **6**, 205-218.
Moreno, T. A., Jappelli, R., Izpisua Belmonte, J. C. and Kintner, C. (2008). Retinoic acid regulation of the Mesp-Ripply feedback loop during vertebrate segmental patterning. *Dev. Biol.* **315**, 317-330.
Morimoto, M., Sasaki, N., Oginuma, M., Kiso, M., Igarashi, K., Aizaki, K., Kanno, J. and Saga, Y. (2007). The negative regulation of Mesp2 by mouse Ripply2 is required to establish the rostro-caudal patterning within a somite. *Development* **134**, 1561-1569.
Muller, C. W. and Herrmann, B. G. (1997). Crystallographic structure of the T domain-DNA complex of the Brachyury transcription factor. *Nature* **389**, 884-888.
Niederreither, K. and Dolle, P. (2008). Retinoic acid in development: towards an integrated view. *Nat. Rev. Genet.* **9**, 541-553.
Niederreither, K., Vermot, J., Schuhbaur, B., Chambon, P. and Dolle, P. (2002). Embryonic retinoic acid synthesis is required for forelimb growth and anteroposterior patterning in the mouse. *Development* **129**, 3563-3574.
Nieuwkoop, P. O. and Faber, J. (1967). A Normal Table of Xenopus laevis (Daudin): A systematical and chronological survey of the development from the fertilized egg till the end of metamorphosis. Amsterdam: North-Holland Publishing Company.
Nowotschin, S., Liao, J., Gage, P. J., Epstein, J. A., Campione, M. and Morrow, B. E. (2006). Tbx1 affects asymmetric cardiac morphogenesis by regulating Pitx2 in the secondary heart field. *Development* **133**, 1565-1573.
Okubo, T., Kawamura, A., Takahashi, J., Yagi, H., Morishima, M., Matsuoka, R. and Takada, S. (2011). Ripply3, a Tbx1 repressor, is required for development of the pharyngeal apparatus and its derivatives in mice. *Development* **138**, 339-348.
Packham, E. A. and Brook, J. D. (2003). T-box genes in human disorders. *Hum. Mol. Genet.* **12** Spec No **1**, R37-R44.
Pan, F. C., Chen, Y., Bayha, E. and Pieler, T. (2007). Retinoic acid-mediated patterning of the pre-pancreatic endoderm in Xenopus operates via direct and indirect mechanisms. *Mech. Dev.* **124**, 518-531.
Papalopulu, N. and Kintner, C. (1996). A posteriorising factor, retinoic acid, reveals that anteroposterior patterning controls the timing of neuronal differentiation in Xenopus neuroectoderm. *Development* **122**, 3409-3418.
Papapetrou, C., Edwards, Y. H. and Sowden, J. C. (1997). The T transcription factor functions as a dimer and exhibits a common human polymorphism Gly-177-Asp in the conserved DNA-binding domain. *FEBS Lett.* **409**, 201-206.
Paroush, Z., Finley, R. L., Jr, Kidd, T., Wainwright, S. M., Ingham, P. W., Brent, R. and Ish-Horowicz, D. (1994). Groucho is required for Drosophila neurogenesis, segmentation, and sex determination and interacts directly with hairy-related bHLH proteins. *Cell* **79**, 805-815.
Pieper, M. and Schlosser, G. (2009). 20-P028 A fatemap of placodes in Xenopus laevis. *Mech. Dev.* **126**, S312-S313.
Radosevic, M., Robert-Moreno, A., Coolen, M., Bally-Cuif, L. and Alsina, B. (2011). Her9 represses neurogenic fate downstream of Tbx1 and retinoic acid signaling in the inner ear. *Development* **138**, 397-408.
Rambaut, A. (2007). FigTree Softare (ed. Institute of Evolutionary Biology, University of Edinburgh).
Rawson, N. E. and LaMantia, A. S. (2006). Once and again: retinoic acid signaling in the developing and regenerating olfactory pathway. *J. Neurobiol.* **66**, 653-676.
Roberts, C., Ivins, S. M., James, C. T. and Scambler, P. J. (2005). Retinoic acid down-regulates Tbx1 expression in vivo and in vitro. *Dev. Dyn.* **232**, 928-938.
Romand, R., Dolle, P. and Hashino, E. (2006). Retinoid signaling in inner ear development. *J. Neurobiol.* **66**, 687-704.
Ryan, A. K., Goodship, J. A., Wilson, D. I., Philip, N., Levy, A., Seidel, H., Schuffenhauer, S., Oechsler, H., Belohradsky, B., Prieur, M. et al. (1997). Spectrum of clinical features associated with interstitial chromosome 22q11 deletions: a European collaborative study. *J. Med. Genet.* **34**, 798-804.
Sacks, B. and Wood, A. (2003). Hearing disorders in children with Down syndrome. *Down Synd. News Upd.* **3**, 38-41.
Schlosser, G. (2006). Induction and specification of cranial placodes. *Dev. Biol.* **294**, 303-351.
Schlosser, G. (2008). Do vertebrate neural crest and cranial placodes have a common evolutionary origin? *BioEssays* **30**, 659-672.
Schlosser, G. and Ahrens, K. (2004). Molecular anatomy of placode development in Xenopus laevis. *Dev. Biol.* **271**, 439-466.
Schlosser, G., Awtry, T., Brugmann, S. A., Jensen, E. D., Neilson, K., Ruan, G., Stammler, A., Voelker, D., Yan, B., Zhang, C. et al. (2008). Eya1 and Six1 promote neurogenesis in the cranial placodes in a SoxB1-dependent fashion. *Dev. Biol.* **320**, 199-214.
Schneider, R. A., Hu, D., Rubenstein, J. L., Maden, M. and Helms, J. A. (2001). Local retinoid signaling coordinates forebrain and facial morphogenesis by maintaining FGF8 and SHH. *Development* **128**, 2755-2767.
Schneider, T. D. and Stephens, R. M. (1990). Sequence logos: a new way to display consensus sequences. *Nucleic Acids Res.* **18**, 6097-6100.
Schulte-Merker, S. and Smith, J. C. (1995). Mesoderm formation in response to Brachyury requires FGF signalling. *Curr. Biol.* **5**, 62-67.
Sharpe, C. R. (1992). Two isoforms of retinoic acid receptor alpha expressed during Xenopus development respond to retinoic acid. *Mech. Dev.* **39**, 81-93.
Shibuya, K., Kudoh, J., Minoshima, S., Kawasaki, K., Asakawa, S. and Shimizu, N. (2000). Isolation of two novel genes, DSCR5 and DSCR6, from Down syndrome critical region on human chromosome 21q22.2. *Biochem. Biophys. Res. Commun.* **271**, 693-698.
Shiotsugu, J., Katsuyama, Y., Arima, K., Baxter, A., Koide, T., Song, J., Chandraratna, R. A. and Blumberg, B. (2004). Multiple points of interaction between retinoic acid and FGF signaling during embryonic axis formation. *Development* **131**, 2653-2667.
Shott, S. R., Joseph, A. and Heithaus, D. (2001). Hearing loss in children with Down syndrome. *Int. J. Pediatr. Otorhinolaryngol.* **61**, 199-205.
Showell, C., Christine, K. S., Mandel, E. M. and Conlon, F. L. (2006). Developmental expression patterns of Tbx1, Tbx2, Tbx5, and Tbx20 in Xenopus tropicalis. *Dev. Dyn.* **235**, 1623-1630.
Shumway-Cook, A. and Woollacott, M. H. (1985). Dynamics of postural control in the child with Down syndrome. *Phys. Ther.* **65**, 1315-1322.
Sinha, S., Abraham, S., Gronostajski, R. M. and Campbell, C. E. (2000). Differential DNA binding and transcription modulation by three T-box proteins, T, TBX1 and TBX2. *Gene* **258**, 15-29.
Song, Y., Hui, J. N., Fu, K. K. and Richman, J. M. (2004). Control of retinoic acid synthesis and FGF expression in the nasal pit is required to pattern the craniofacial skeleton. *Dev. Biol.* **276**, 313-329.
Stratford, T., Logan, C., Zile, M. and Maden, M. (1999). Abnormal anteroposterior and dorsoventral patterning of the limb bud in the absence of retinoids. *Mech. Dev.* **81**, 115-125.
Streit, A. (2007). The preplacodal region: an ectodermal domain with multipotential progenitors that contribute to sense organs and cranial sensory ganglia. *Int. J. Dev. Biol.* **51**, 447-461.
Uniprot Consortium (2009). The Universal Protein Resource (UniProt) 2009. *Nucleic Acids Res.* **37**, D169-D174.
Villanueva, S., Glavic, A., Ruiz, P. and Mayor, R. (2002). Posteriorization by FGF, Wnt, and retinoic acid is required for neural crest induction. *Dev. Biol.* **241**, 289-301.
Vitelli, F., Viola, A., Morishima, M., Pramparo, T., Baldini, A. and Lindsay, E. (2003). TBX1 is required for inner ear morphogenesis. *Hum. Mol. Genet.* **12**, 2041-2048.
Whitfield, T. T., Granato, M., van Eeden, F. J., Schach, U., Brand, M., Furutani-Seiki, M., Haffter, P., Hammerschmidt, M., Heisenberg, C. P., Jiang, Y. J. et al. (1996). Mutations affecting development of the zebrafish inner ear and lateral line. *Development* **123**, 241-254.
Wilson, V. and Conlon, F. L. (2002). The T-box family. *Genome Biol.* **3**, REVIEWS3008.
Wuang, Y. P. and Su, C. Y. (2011). Correlations of sensory processing and visual organization ability with participation in school-aged children with Down syndrome. *Res. Dev. Disabil.* **32**, 2398-2407.
Zhang, L., Zhong, T., Wang, Y., Jiang, Q., Song, H. and Gui, Y. (2006). TBX1, a DiGeorge syndrome candidate gene, is inhibited by retinoic acid. *Int. J. Dev. Biol.* **50**, 55-61.